

Colossal magnetoelastic effects at the phase transition of $(\text{La}_{0.6}\text{Pr}_{0.4})_{0.7}\text{Ca}_{0.3}\text{MnO}_3$

M. Michelmann, V. Moshnyaga, and K. Samwer

I. Physikalisches Institut, Georg-August Universität Göttingen, Friedrich-Hund-Platz 1, D-37077 Göttingen, Germany

(Received 23 May 2011; revised manuscript received 13 December 2011; published 23 January 2012)

$(\text{La}_{0.6}\text{Pr}_{0.4})_{0.7}\text{Ca}_{0.3}\text{MnO}_3$ was characterized by means of ultrasound velocity and attenuation to study the temperature and magnetic field dependence of the elastic constants and to gain an insight into the metamagnetic transition. The metal-insulator and ferromagnetic-paramagnetic transitions are reflected in the behavior of the elastic constants due to strong electron-phonon and spin-phonon interactions. A hysteresis in elastic behavior and metamagnetism hints toward first-order nature of the phase transition. A softening of bulk modulus at the ferromagnetic transition for magnetic fields $\mu_0 H > 2$ T was attributed to a coupling between the lattice and spin fluctuations. This softening peaks at a certain temperature $T^* \approx 215$ K and field $\mu_0 H^* \approx 4$ T, which could be an indication of a critical end point of the ferromagnetic transition.

DOI: [10.1103/PhysRevB.85.014424](https://doi.org/10.1103/PhysRevB.85.014424)

PACS number(s): 75.80.+q, 75.30.Kz, 62.65.+k

I. INTRODUCTION

Materials that show a ferromagnetic phase transition of the first order like $\text{Gd}_5(\text{Si}_2\text{Ge}_2)$, $\text{MnAs}_{1-x}\text{Sb}_x$, and $\text{La}(\text{Fe},\text{Si})_{13}$ have attracted much attention due to large magnetocaloric effects at the vicinity of the transition that offers the possibility of magnetic refrigerant applications.^{1–3} Giant entropy changes at the metamagnetic transition are achieved in systems with a strong coupling between spin and lattice degrees of freedom, so a structural transition is induced by magnetic field application.³ $(\text{La}_{1-y}\text{Pr}_y)_{1-x}\text{Ca}_x\text{MnO}_3$ perovskite manganese oxides have long been the subject of intensive study due to the interplay of double exchange and electron-phonon coupling of the Jahn-Teller type that can lead to either ferromagnetic metallic (FM) or charge-ordered antiferromagnetic insulating (CO) ground states.⁴ These competing interactions give rise to a long-scale FM/CO phase coexistence, which was believed to be the reason for colossal magnetoresistance (CMR) effect.^{5,6} For carrier doping $x \approx \frac{1}{3}$ a ferromagnetic phase transition of the first-order type has been reported.^{4,7,8} V. S. Amaral *et al.*⁹ revealed a critical point of the first-order transition in $\text{La}_{0.67}\text{Ca}_{0.33}\text{MnO}_3$ by means of isothermal magnetization measurements. With increasing Pr concentration this transition is accompanied by pronounced thermal and field hysteresis as well as by metamagnetism. A strong electron-phonon coupling has been proposed to be the reason for the first-order transition.^{10,11} The direct connection between the lattice and electrons is displayed by changes in the lattice properties at the ferromagnetic phase transition. For $\text{La}_{2/3}\text{Ca}_{1/3}\text{MnO}_3$ an anomalous thermal expansion with a sharp volume contraction of about $\approx 0.1\%$ ¹² and a steep increase of the sound velocity^{13–16} at the metal-to-insulator transition have been observed.

II. EXPERIMENTAL DETAILS

Here we report on the study of sound velocity in polycrystalline $(\text{La}_{0.6}\text{Pr}_{0.4})_{0.7}\text{Ca}_{0.3}\text{MnO}_3$ (LPCMO) prepared by a solid-state reaction from commercial metal-organic precursors. Stoichiometric amounts of La, Pr, Ca, and Mn acetylacetonates were dissolved in dimethylformamide and the solution was pipetted onto a dish at a temperature of 300°C under steady stirring, whereas the solvent was vaporized. The

remaining crystallized powder was ground, annealed in air at 1000°C for 12 h, and pressed into a pellet under a pressure of 100–300 MPa. The specimen was annealed in several steps with increasing temperatures up to 1400°C and intermediate grindings and cooled down to room temperature at a rate of $3^\circ\text{C}/\text{min}$. The cylindrical sample was 5 mm in diameter and 3.46 mm thick and was hand lapped to obtain a plane parallelism of $50\text{ }\mu\text{m}$ or better. X-ray powder diffraction confirms a single spurious cubic perovskite structure with no detectable secondary phase. The mean pseudocubic lattice parameter was found to be $a = 0.3860(2)$ nm. The magnetization of the sample was measured using a commercial superconducting quantum interference device magnetometer (Quantum Design).

Ultrasound velocity measurements have been carried out in a temperature range, $T = 40\text{--}300$ K, and in external magnetic fields, $\mu_0 H = 0\text{--}7$ T, by means of a conventional pulse-echo technique. Using a standard four-probe method electrical resistance was measured simultaneously with ultrasound velocity. During the temperature sweep, a cooling and heating rates of $2\text{ K}/\text{min}$ were applied. Piezoelectric transducers (PZT-5A) at 12 and 14 MHz fundamental frequencies were bonded to the sample with UHU universal adhesive. The transducer excites broadband longitudinal and transversal ultrasound pulses by application of 20-ns-long needle voltage pulses and converts the back wall echoes to an electric signal that is acquired and digitized after preamplification by a 1-GHz oscilloscope. The maximum of the cross-correlation of two successive echoes provides the time of flight t of the ultrasound wave through the sample and, therefore, the sound velocity $v = 2l/t$ with the sample length l .¹⁷ A polycrystalline ceramic sample can be treated as an isotropic elastic material with two independent elastic constants, e.g., the bulk modulus K and shear modulus G . Therefore, two different sound velocities v_l and v_t of longitudinal and transversal waves, respectively, can be determined. They are related to the elastic constants via

$$K = \rho \left(v_l^2 - \frac{4}{3} v_t^2 \right), \quad (1a)$$

$$G = \rho v_t^2, \quad (1b)$$

with the mass density ρ . Using a pycnometer with distilled water as working fluid the density was estimated to be $\rho =$

5.756(5) g/m³, which indicate a pore volume fraction of about 7%.

III. RESULTS AND DISCUSSION

Figure 1 shows the temperature dependence of the resistance R . A maximum at an insulator-metal transition temperature, $T_{MI} = 191$ K, as well as a thermal hysteresis in the temperature range $T = 70$ –200 K were observed at zero magnetic field. For magnetic fields $\mu_0 H \geq 2$ T the thermal hysteresis vanishes and the metal-insulator transition is shifted to higher temperatures at a rate of ≈ 8 K/T. Figures 2(a) and 2(b) show the measured magnetization of LPCMO as a function of temperature, T , and magnetic field, H , respectively. A sharp increase in magnetization, observed at the Curie point $T_C = 188$ K, is accompanied by a thermal hysteresis in the range $T = 165$ –200 K, indicating a first-order phase transition in agreement with previous reports on LPCMO.^{4,5} The isothermal magnetization in Fig. 2(b) reveals a ferromagnetic behavior for $T < T_C$ with a saturation magnetization close to the expected value of $M_S \approx 3.7 \mu_B$ per Mn ion at 10 K. Between 190 and 220 K the $M(H)$ curves show an inflection point, indicating a metamagnetic transition from a paramagnetic to a ferromagnetic state. Since no discontinuities and hysteresis could be observed in isothermal $M(H)$ curves for $T > 200$ K, we cannot distinguish between a true phase transition and a crossover only from magnetization measurements.

The temperature dependence of bulk and shear modulus evaluated from Eqs. (1a) and (1b) at magnetic fields of $\mu_0 H = 0, 2, 3, 4, 5$ and 7 T are shown in Figs. 3(a) and 3(b). In a zero field both elastic constants show a steplike hardening $\Delta K/K \approx 3\%$ and $\Delta G/G \approx 15\%$ in a temperature range $T = 180$ –195 K, which correlates to the jump of the magnetization at T_C and the drop of resistivity at the metal-insulator transition. This observation agrees with previous results on $\text{La}_{2/3}\text{Ca}_{1/3}\text{MnO}_3$ (LCMO)^{13–15} and $\text{La}_{2/3}\text{Sr}_{1/3}\text{MnO}_3$ (LSMO),¹⁵ which show an increase of transversal and longitudinal sound velocity close to T_C , which corresponds

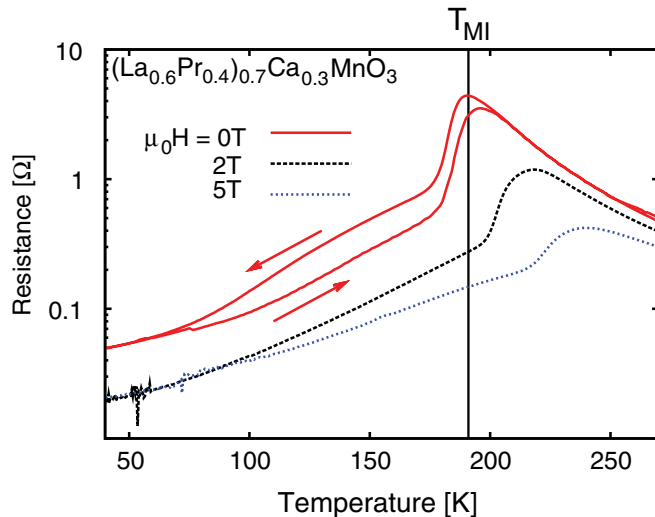


FIG. 1. (Color online) Temperature dependence of the resistance R in semilogarithmic scale for magnetic fields $\mu_0 H = 0, 2$, and 5 T.

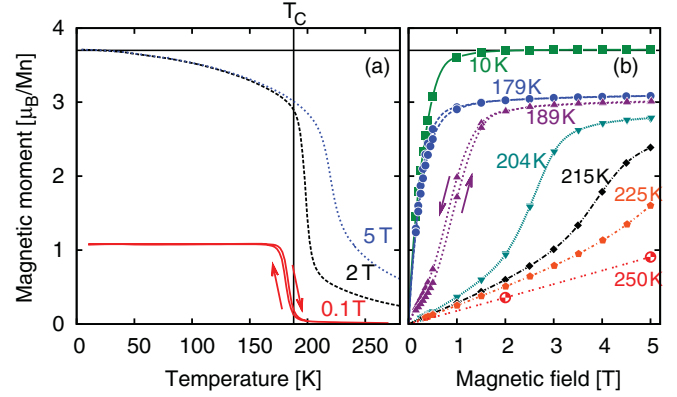


FIG. 2. (Color online) Magnetization M as a function of temperature (a) and magnetic field (b) of $(\text{La}_{0.6}\text{Pr}_{0.4})_{0.7}\text{Ca}_{0.3}\text{MnO}_3$ for different external fields $\mu_0 H = 0, 2$, and 5 T and temperatures $T = 10, 179, 189, 215, 225$, and 250 K, respectively. The isothermal $M(H)$ curve at $T = 250$ K was extracted from the $M(T)$ curves. Solid black lines indicate the full magnetic moment of $3.7 \mu_B$ per ion. Curie temperature $T_C = 188$ K was estimated by linear extrapolation of the magnetization onset.

to changes $\Delta G/G \approx 10$ –14% and $\Delta K/K \approx 5\%$ of elastic moduli. Although no temperature hysteresis in the elastic constants could be determined from the heating and cooling curves, the magnetic field hysteresis effects were observed at isothermal measurements as described below. With increasing field the rise in shear modulus [see Fig. 3(b)] is shifted to higher temperatures and get broadened, following the behavior of the magnetization and resistivity. Therefore, the shear stiffness shows a dramatic sensitivity to an external magnetic field at T_C , so a hardening, $\Delta G/G \approx 10\%$, is achieved for $\mu_0 H \approx 2$ T.

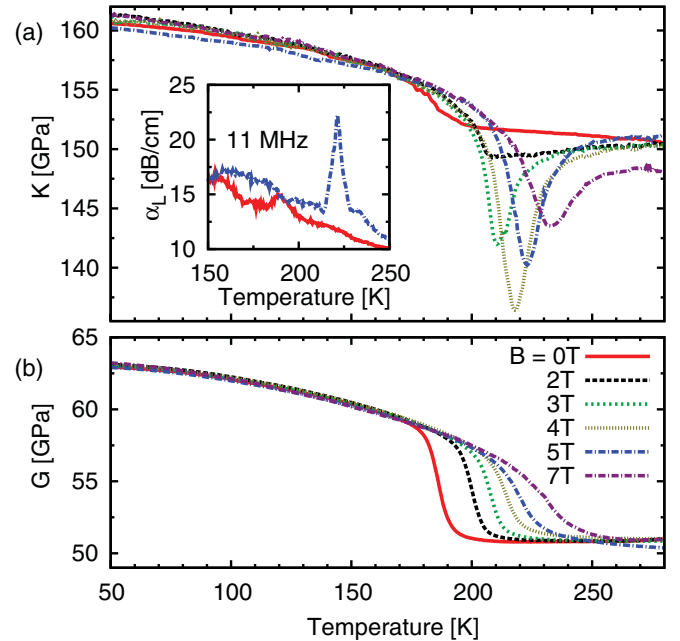


FIG. 3. (Color online) Bulk modulus K (a) and shear modulus G (b) of $(\text{La}_{0.6}\text{Pr}_{0.4})_{0.7}\text{Ca}_{0.3}\text{MnO}_3$ as a function of temperature for different magnetic fields $\mu_0 H = 0, 2, 3, 4, 5$, and 7 T. (Inset) Longitudinal sound attenuation at a frequency of 11 MHz is shown for $\mu_0 H = 0$ T (red) and 5 T (blue).

In contrast to shear stiffness, the temperature anomaly in bulk modulus is enhanced by application of a magnetic field. The $K(T)$ curves reveal an additional feature for $\mu_0 H > 2$ T, whereby the elastic constant shows a pronounced minimum, $\Delta K/K \approx -11\%$ for $\mu_0 H = 4$ T, in the vicinity of T_C . As shown in the inset of Fig. 3(a) this softening is accompanied by a peak in the attenuation of the longitudinal waves with an increase, $\Delta\alpha_L/\alpha_L \approx 65\%$, at 11 MHz and $\mu_0 H = 5$ T relative to the background. A much weaker minimum in the bulk modulus of the order of $\Delta K/K \approx -2\%$ was also reported for $\text{La}_{1-x}\text{Ca}_x\text{MnO}_3$, $x = 0.25$ and 0.33 , in the absence of an external magnetic field.^{14,16} According to Belevtsev *et al.*,¹⁶ this anomaly increases considerably in magnitude and becomes broader through application of a magnetic field. It is similar to our results on LPCMO.

The origin of the elastic hardening at T_C has been suggested by J. D. Lee *et al.* to be the electron-phonon interaction due to the change in electron screening at the metal-insulator transition.¹⁸ The increase of the one-electron bandwidth in the ferromagnetic phase due to double exchange cause a less screened ionic core potential and, therefore, a higher elastic stiffness.¹⁹ Since double-exchange interaction is common for LPCMO, LCMO, and LSMO, the electron screening can be an explanation for the elastic hardening in all these materials. However, the predicted change in the sound velocity¹⁸ is almost an order of magnitude lower than that observed here. The development of correlated polarons of the CE type in $\text{Pr}_{0.65}\text{Ca}_{0.35}\text{MnO}_3$ (PCMO) far above the charge-ordering temperature $T_{CO} = 229$ K is known to cause a substantial softening of about 10% of the $(C_{11} - C_{12})/2$ shear mode between 400 K and T_{CO} .²⁰ We observed no significant softening of shear stiffness as the temperature was lowered from 300 to 220 K, which indicates that polaronic correlations have only a minor effect on the elastic properties.

Figures 4(a) and 4(b) show the behavior of isothermal resistance R and shear modulus G as a function of magnetic field for temperatures $T = 189$ K and 179 K after a zero-field cooling. The field-induced changes of both resistance and shear modulus display a reversible hysteresis loop and an

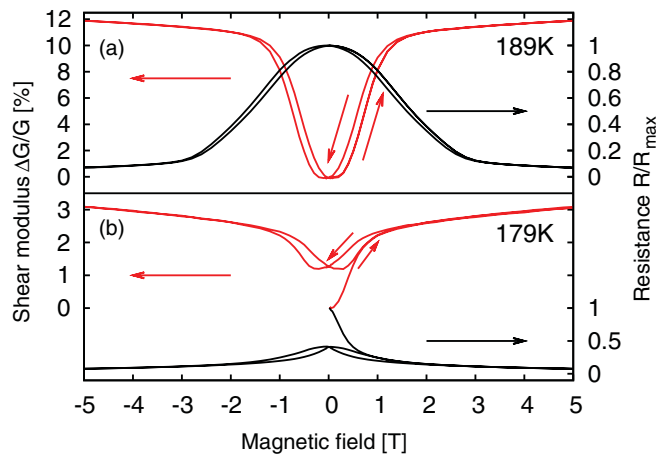


FIG. 4. (Color online) Relative change of shear modulus G and normalized resistance R of $(\text{La}_{0.6}\text{Pr}_{0.4})_{0.7}\text{Ca}_{0.3}\text{MnO}_3$ as a function of magnetic field at temperatures of $T = 179$ K and $T = 189$ K after zero-field cooling.

initial curve with an irreversible lowering of the resistance and a remanent hardening of elastic stiffness after the external field is removed. The $R(B)$ curve resembles the tunneling magnetoresistance (TMR) of powder compacts,²¹ but for a temperature $T = 100$ K, far below the Curie point, the reversible hysteresis loops in the resistance vanish (not shown here) although the TMR ratio should increase with decreasing temperature due to the enhanced spin polarization.²² Due to linear magnetostriction also the elastic constants depend on the magnetic domain structure, so elastic stiffness is lowered in the demagnetized state, since domain rotation and domain wall motion induced by mechanical stress leads to an extra strain.²³ This so-called ΔE effect is common to all ferromagnetic materials and can lead to a reduction of Young's modulus E of more than 50% in amorphous ribbons.²⁴ But the magnetic field hysteresis of the elastic constants appears for LPCMO only in a narrow temperature range $170 \text{ K} \leq T \leq 205 \text{ K}$ close to the Curie point. Furthermore, neither bulk nor shear modulus show a considerable magnetic field dependence below $T = 170$ K (less than 0.8% change of the elastic constants in a field of $\mu_0 H = 5$ T), so the ΔE effect can have only a small influence. For these reasons we attribute the field hysteresis of both resistance and elastic constants mainly to a magnetic field-induced insulator-metal transition. In the widely accepted phase separation scenario the FM phase develops continuously as temperature is lowered below T_C , whereby application of a low magnetic field can transform the remaining insulating fraction into the FM state.⁶ The insulating phase undergoes a field-induced first-order transition, whereby the system tends to stay in the FM state as the field is lowered back, leading to a hysteresis of the metallic fraction, which is directly connected with the resistance and elastic constants.

In Figs. 5(a) and 5(b) the isothermal $G(H)$, $K(H)$, and $\alpha_L(H)$ curves are shown for temperatures $T = 205$, 215 , and

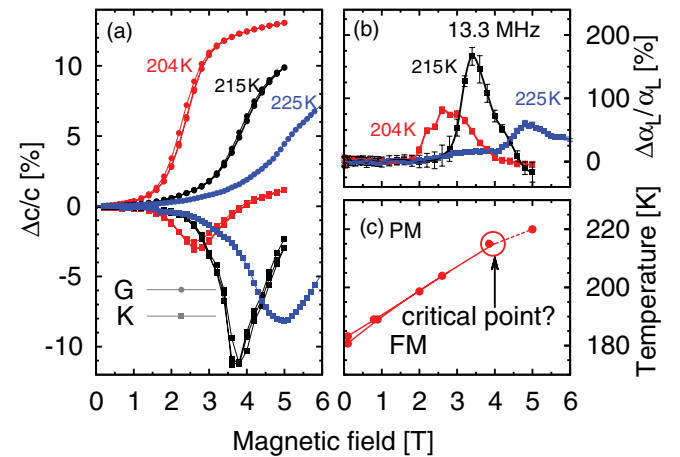


FIG. 5. (Color online) Magnetic field dependence of (a) the elastic constants K and G and (b) the longitudinal sound attenuation α_L at a frequency of 13.3 MHz for temperatures $T = 204$, 215 , and 225 K of $(\text{La}_{0.6}\text{Pr}_{0.4})_{0.7}\text{Ca}_{0.3}\text{MnO}_3$. (c) Magnetic phase diagram for LPCMO: Dots are points of the paramagnetic-ferromagnetic transition or crossover marked by inflection points in the $M(T)$ and $M(H)$ curves. The bifurcation of the transition lines at fields $\mu_0 H \leq 2$ T corresponds to the observed temperature and field hysteresis. The first-order transition line may possibly end in a critical point at around $T^* \approx 215$ K and $\mu_0 H^* \approx 4$ T.

225 K. As shown in Fig. 2(b), the metamagnetic transition is accompanied, on the one hand, by a hardening of the shear modulus G and, on the other hand, by a minimum in the bulk modulus K and a maximum of the longitudinal attenuation α_L that appears both for fields higher than 2 T. Although the behavior of the bulk modulus resembles the ΔE effect of amorphous ferromagnetic ribbons,²⁴ a redistribution of magnetic domains cannot lead to a volume expansion and has, therefore, no influence on the compressibility.²³ Prior ultrasound measurements on PCMO revealed, as a function of magnetic field for $T = 220$ K, a comparable minimum of longitudinal velocity that alters to a steplike jump for lower temperatures.²⁵ But, in contrast to our results, the authors attributed this softening of longitudinal velocity to a melting of the charge-ordered phase that is not present in our case. But, very similar to our results, a dip in the longitudinal sound velocity $v_l(H)$ was found in $\text{La}_{0.75}\text{Ca}_{0.25}\text{MnO}_3$ at the magnetic field-induced paramagnetic-ferromagnetic transition.¹⁶

This minimum of the bulk modulus at the magnetic transition may be originated from spin-phonon coupling because of the strain modulation of the exchange energy.^{26,27} Since the exchange interaction couples virtually only to the changes of interatomic distances, which are first-order quantities in the compression but second-order quantities in shear deformation, only changes in the bulk modulus are expected at the Curie temperature. In agreement with our results, a sharp dip in the sound velocity and an attenuation peak for longitudinal waves have been reported for ferromagnets like Ni ²⁸ and Gd ²⁷ and also for antiferromagnets like RbMnF_3 ²⁹ and FeCl_2 ³⁰ at the magnetic transition. We observe in LPCMO a much larger velocity drop $|\Delta v_l/v_l| \approx 6\%$ at T_C than that reported for most of the other magnetic systems (for example, $|\Delta v_l/v_l| \approx 0.2\%$ is shown for Gd ²⁷ and $|\Delta v_l/v_l| \approx 1.2\%$ for FeCl_2).³⁰ Pippard's equations for second-order phase transitions yield a relation for the corresponding bulk modulus softening^{29,31} as follows:

$$\frac{\Delta K}{K} = -\frac{\Delta C_p}{TV} K \left(\frac{dT_C}{dp} \right)^2 \quad (2)$$

with the spin heat capacity ΔC_p and the volume V . Due to the large pressure dependence of Curie temperature for LPCMO ($dT_C/dp \approx 14$ K/GPa),³² a softening of $\Delta K/K \approx -11\%$ can be expected for a typical magnetic heat contribution of $\Delta C_p \approx 25$ J/mol K in CMR manganites,³³ in excellent agreement with our results.

The dominant mechanism for the anomalies in sound propagation and attenuation for the band ferromagnets has been assigned to spin fluctuations, which diverge in length scales and relaxation times at the second-order phase transition. This leads to a random force on the lattice and to a transfer of the energy from the sound wave to the spin system.²⁷ But in LPCMO a first-order phase transition is present, so spin fluctuations are limited at the Curie point. This explains the absence of the softening in bulk modulus and the longitudinal attenuation peak without an applied magnetic field in Fig. 3(a). The minimum in the bulk modulus appears only with application of an external magnetic field $\mu_0 H > 2$ T. Belevtsev *et al.* found in $\text{La}_{0.75}\text{Ca}_{0.25}\text{MnO}_3$ also an enhancement of the longitudinal sound velocity drop under influence of a magnetic field and

claimed that the phase transition of first order becomes second order for this reason.¹⁶ An applied magnetic field drives the first-order ferromagnetic transition to a critical end point that represents a point of a continuous transition and exhibits a divergence in a differential spin susceptibility, $\chi = dM/dH$, and, therefore, leads to fluctuations on all length and times scales.³⁴ Scale-invariant fluctuations of the order parameter gives rise to a novel behavior like, e.g., the critical opalescence for the gas-liquid transition. In our case, the softening of the bulk modulus and the attenuation peak are maximal at the temperature, $T^* \approx 215$ K, and magnetic field, $\mu_0 H^* \approx 4$ T. For this reason, we propose a phase diagram shown in Fig. 5(c) with a possible critical end point at (T^*, H^*) . In a region around this point an anomalous behavior of longitudinal wave propagation and attenuation emerges due to an enhanced amount of spin fluctuations at the ferromagnetic transition or crossover.

Similar enhancement of the longitudinal sound velocity softening by application of a magnetic field were found near the tricritical point of FeCl_2 .³⁰ Furthermore, the minimum in sound velocity vanishes as the transition changes from second to first order in FeCl_2 . Anomalous sound velocity have been also reported for the critical end point of the insulator-metal transition in the layered organic superconductor $\kappa\text{-(BEDT-TTF)}_2\text{Cu}[\text{N}(\text{CN})_2]\text{Cl}$, which corresponds to a predicted compressibility divergence.³⁵

La(Fe, Si)_{13} might be a very interesting material for studying magnetoelastic effects around a ferromagnetic critical end point due to its common features with LPCMO. It undergoes a paramagnetic-ferromagnetic transition of the first order that is accompanied by a large volume expansion on the order of 1%–2%.³⁶ Melt-spun $\text{LaFe}_{11.6}\text{Si}_{1.4}$ exhibits a large entropy change and a low thermal and magnetic field hysteresis at the metamagnetic transition and became, therefore, a promising material for magnetic refrigerant applications.³ A sharp heat capacity peak related to spin fluctuations was observed at its metamagnetic transition in the vicinity of its critical end point. Since the magnetic heat capacity couples directly to the bulk modulus [see Eq. (2)], a large rise of the compressibility at the transition can be expected. Resistivity data of $\text{LaFe}_{11.8}\text{Si}_{1.2}$ indicates a large decrease of bulk modulus by about 50% near its Curie point.³⁷ Furthermore, the adiabatic temperature change in the vicinity of T_C displays a magnetic field hysteresis with both an initial curve and a closed hysteresis loop that corresponds to remanent and reversible volume changes induced by the applied field.³⁸ This hysteresis behavior resembles the field dependence of resistance and shear modulus in LPCMO shown in Fig. 4.

IV. CONCLUSIONS

In summary, we have studied the ferromagnetic phase transition in the bulk LPCMO by means of ultrasound velocity and attenuation. Magnetic field hysteresis effects and metamagnetism related to the first-order nature of the phase transition as well as the electronic phase separation are reflected in the behavior of elastic constants. Close to the Curie temperature application of modest magnetic fields leads to a hardening of shear stiffness and to a softening of

bulk modulus of the order of 10%. The observed hardening of elastic constants in the metallic phase and a minimum of the bulk modulus at the transition point can be attributed to the electron-phonon and spin-phonon coupling, respectively. The latter coupling gives an insight to spin fluctuations and hints toward a critical end point of the ferromagnetic transition.

ACKNOWLEDGMENTS

The authors thank W. Arnold for fruitful discussions and helpful advice for the ultrasound measurement. This work was supported by SFB 602 of the Deutsche Forschungsgemeinschaft (TP A2) and by IFOX of the European Community's 7th Framework Programme.

- ¹V. K. Pecharsky and K. A. Gschneidner Jr., *Phys. Rev. Lett.* **78**, 4494 (1997).
- ²H. Wada, T. Morikawa, K. Taniguchi, T. Shibata, Y. Yamada, and Y. Akishige, *Physica B* **328**, 114 (2003).
- ³K. Morrison, J. Lyubina, J. D. Moore, A. D. Caplin, K. G. Sandeman, O. Gutfleisch, and L. F. Cohen, *J. Phys. D: Appl. Phys.* **43**, 132001 (2010).
- ⁴H. Y. Hwang, S.-W. Cheong, P. G. Radaelli, M. Marezio, and B. Batlogg, *Phys. Rev. Lett.* **75**, 914 (1995).
- ⁵M. Uehara, S. Mori, C. H. Chen, and S.-W. Cheong, *Nature* **399**, 560 (1999).
- ⁶J. Burgu, M. Mayr, V. Martin-Mayor, A. Moreo, and E. Dagotto, *Phys. Rev. Lett.* **87**, 277202 (2001).
- ⁷D. Kim, B. Revaz, B. L. Zink, F. Hellman, J. J. Rhyne, and J. F. Mitchell, *Phys. Rev. Lett.* **89**, 227202 (2002).
- ⁸Y. Tomioka, A. Asamitsu, H. Kuwahara, Y. Moritomo, and Y. Tokura, *Phys. Rev. B* **53**, R1689 (1996).
- ⁹V. S. Amaral, J. P. Araújo, Y. G. Pogorelov, J. B. Sousa, P. B. Tavares, J. M. Vieira, P. A. Algarabel, and M. R. Ibarra, *J. Appl. Phys.* **93**, 7646 (2003).
- ¹⁰A. S. Alexandrov and A. M. Bratkovsky, *Phys. Rev. Lett.* **82**, 141 (1999).
- ¹¹J. A. Vergés, V. Martín-Mayor, and L. Brey, *Phys. Rev. Lett.* **88**, 136401 (2002).
- ¹²J. M. De Teresa, M. R. Ibarra, P. A. Algarabel, C. Ritter, C. Marquina, J. Blasco, J. García, A. del Moral, and Z. Arnold, *Nature* **386**, 256 (1997).
- ¹³A. P. Ramirez, P. Schiffer, S.-W. Cheong, C. H. Chen, W. Bao, T. T. M. Palstra, P. L. Gammel, D. J. Bishop, and B. Zegarski, *Phys. Rev. Lett.* **76**, 3188 (1996).
- ¹⁴C. Zhu, R. Zheng, J. Su, and J. He, *Appl. Phys. Lett.* **74**, 3504 (1999).
- ¹⁵J. Mira, J. Rivas, A. Moreno-Gobbi, M. Pérez Macho, G. Paolini, and F. Rivadulla, *Phys. Rev. B* **68**, 092404 (2003).
- ¹⁶B. I. Belevtsev, G. A. Zvyagina, K. R. Zhekov, I. G. Kolobov, E. Y. Beliaev, A. S. Panfilov, N. N. Galtsov, A. I. Prokhvatilov, and J. Fink-Finowicki, *Phys. Rev. B* **74**, 054427 (2006).
- ¹⁷D. Marioli, C. Narduzzi, C. Offelli, D. Petri, E. Sardini, and A. Taroni, *IEEE Trans. Instrum. Meas.* **41**, 93 (1992).
- ¹⁸J. D. Lee and B. I. Min, *Phys. Rev. B* **55**, 12454 (1997).
- ¹⁹D. J. Kim, *Phys. Rep.* **171**, 129 (1988).
- ²⁰H. Hazama, T. Goto, Y. Nemoto, Y. Tomioka, A. Asamitsu, and Y. Tokura, *Phys. Rev. B* **69**, 064406 (2004).
- ²¹J. M. D. Coey, *Philos. Trans. R. Soc. London A* **356**, 1519 (1998).
- ²²A. H. Davis, J. M. MacLaren, and P. LeClair, *J. Appl. Phys.* **89**, 7567 (2001).
- ²³E. W. Lee, *Rep. Prog. Phys.* **18**, 184 (1955).
- ²⁴N. P. Kobelev, Y. M. Soifer, V. G. Shteinberg, and Y. B. Levin, *Phys. Status Solidi A* **102**, 773 (1987).
- ²⁵S. Seiro, G. Reményi, M. Saint-Paul, H. R. Salva, A. Ghilarducci, P. Monceau, and P. Léjay, *Mat. Sci. Eng. A* **370**, 384 (2004).
- ²⁶B. Lüthi, *Physical Acoustics in the Solid State* (Springer, Berlin, 2005).
- ²⁷I. K. Kamilov and K. K. Aliev, *Phys. Usp.* **41**, 865 (1998).
- ²⁸B. Golding and M. Barmatz, *Phys. Rev. Lett.* **23**, 223 (1969).
- ²⁹B. Lüthi, T. J. Moran, and R. J. Pollina, *J. Phys. Chem. Solids* **31**, 1741 (1970).
- ³⁰A. S. G. Gorodetsky and V. Volterra, *Sol. St. Comm.* **25**, 1129 (1978).
- ³¹G. Hausch, *Phys. Stat. Sol.* **29**, K149 (1975).
- ³²H. Y. Hwang, T. T. M. Palstra, S.-W. Cheong, and B. Batlogg, *Phys. Rev. B* **52**, 15046 (1995).
- ³³D. Kim, B. L. Zink, F. Hellman, and J. M. D. Coey, *Phys. Rev. B* **65**, 214424 (2002).
- ³⁴H. Yamada, *Phys. Rev. B* **47**, 11211 (1993).
- ³⁵D. Fournier, M. Poirier, M. Castonguay, and K. D. Truong, *Phys. Rev. Lett.* **90**, 127002 (2003).
- ³⁶L. Jia, J. Liu, J. R. Sun, H. W. Zhang, F. X. Hu, C. Dong, G. H. Rao, and B. G. Shen, *J. Appl. Phys.* **100**, 123904 (2006).
- ³⁷T. T. M. Palstra, J. A. Mydosh, G. J. Nieuwenhuys, and A. M. van der Kraan, *J. Mag. Mag. Mat.* **36**, 290 (1983).
- ³⁸J. Liu, M. Krautz, K. Skokov, T. G. Woodcock, and O. Gutfleisch, *Act. Mat.* **59**, 3602 (2011).